Ali, M.; Ahmed, I.; Ramirez Hoyos, P.; Nasir, S.; Mafe, S.; Niemeyer, CM.; Ensinger, W. (2017). A redox-sensitive nanofluidic diode based on nicotinamide-modified asymmetric nanopores. Sensors and Actuators B Chemical. 240:895-902. https://doi.org/10.1016/j.snb.2016.09.061

A redox-sensitive nanofluidic diode based on nicotinamide-modified asymmetric nanopores

Mubarak Ali,[a,b]* Ishtiaq Ahmed,[c] Patricio Ramirez,[d] Saima Nasir,[a] Salvador Mafe,[e] Christof M. Niemeyer,[c] and Wolfgang Ensinger[a]

[a]*Technische Universität Darmstadt, Fachbereich Material- u. Geowissenschaften, Fachgebiet Materialanalytik, Alarich-Weiss-Str. 2, D-64287 Darmstadt, Germany*

[b]*GSI Helmholtzzentrum für Schwerionenforschung, Planckstr. 1, D-64291 Darmstadt, Germany*

[c]*Karlsruhe Institute of Technology (KIT), Institute for Biological Interfaces (IBG-1), Hermann-von-Helmholtz-Platz, D-76344 Eggenstein-Leopoldshafen, Germany*

[d]*Departament de Física Aplicada, Universitat Politécnica de València, E-46022 València, Spain*

[e]*Departament de Física de la Tierra i Termodinàmica, Universitat de València, E-46100 Burjassot, Spain.*

* Corresponding author: E-mail address: M.Ali@gsi.de (M. Ali)

Abstract

We demonstrate a redox-sensitive nanofluidic diode whose ion rectification is modulated by the oxidation and reduction of chemical moieties incorporated on its surface. To achieve this goal, we have first synthesized the chemical compounds 1-(4-aminobutyl)-3-carbamoylpyridin-1-ium (Nic-BuNH_2) and 3-carbamoyl-1-(2,4-dinitrophenyl)pyridinium (Nic-DNP). Then, the surface of track-etched single asymmetric nanopores is decorated with the redox-sensitive Nic-BuNH_2 and Nic-DNP molecules using carbodiimide coupling chemistry and Zincke reaction, respectively. The success of the modification reactions is monitored through the changes in the current–voltage (*I–V*) curves prior to and after pore functionalization. Upon exposing

the modified pore to solutions of hydrogen peroxide (oxidizing agent) and sodium dithionite (reducing agent) the surface charge is reversibly modulated from positive to neutral, leading to measurable changes in the electronic readout of ion current passing through the nanopore. On oxidation, the quaternary nicotinamide units impart positive charge to the pore surface, resulting in the ion current rectification (anion-selective pore). On the contrary, the complementary reduced dihydronicotinamide moieties resulted in the loss of surface charge and ohmic behaviour (non-selective pore). The experimental results are further theoretically described by using Poisson-Nernst-Planck equations.

Keywords: synthetic nanopores; redox reaction; nicotinamide; current rectification; surface functionalization; track-etching.

1. Introduction

Ion channels and nanopores have received much attention because of their unique transport properties. In living organisms, ion channels regulate the flow of ions (e.g., Na^+, K^+, and Cl^-) and small organic molecules into and out of the cell membrane to facilitate the chemical and electrical communication with the extracellular environment. Biological pores are highly selective and can discriminate between ions with similar size and same charge [1]. Therefore, they are frequently employed as model systems to investigate transport phenomena at the nanoscale [2, 3]. Among the various protein pores, the α-hemolysin self-assembled in a lipid bilayer has been extensively used for the detection and analysis of biomolecules [4, 5]. However, the fragility and sensitivity of the embedding lipid bilayer towards harsh

conditions (temperature, pH and salt concentrations) restrain its use for more practical purposes. On the contrary, robust synthetic nanopores have recently attracted a great deal of interest in the area of nano/biotechnology. The structural (size and shape) and chemical (fixed charges) characteristics of synthetic nanopores have some similarities with their biological counterparts [6-8]. Asymmetric nanopores display ionic transport properties such as ion current rectification, current gating, and ion selectivity [9-12].

The electrical charge on the pore surface is one of the key parameters that determine the ion current rectification in conical nanopores [9-11]. To date, a variety of responsive molecules and functional groups that respond to external stimuli such as ions [13, 14], biomolecules [15-18], light [19-22], pH [3, 23-25], temperature [26, 27] and combinations of pH and temperature [28, 29] have been immobilized onto the pore surface. Upon the application of an external stimulus, the modified pore undergoes changes in the effective diameter and surface charge polarity, resulting in the variation of ionic flux across the membrane. Recently, ionic permeation across membranes has also been modulated through redox reactions occurring in nanoconfined geometries.[30-37] For this purpose, a variety of redox sensitive moieties have been functionalized on the inner pore walls. For example, Vansco and co-workers have demonstrated the fabrication of redox-responsive porous polyelectrolyte membranes by the complexation of poly(ferrocenylsilane) based poly(ionic liquid)s and poly(acrylic acid) [36]. Miller and Martin have demonstrated the tuning of electroosmotic flow through carbon nanotube membranes via depositing a thin film of redox polymer poly(vinylferrocene) on the inner walls [34]. Recently, Mitta el al, miniaturized a redox sensitive nanofluidic diode based on an asymmetric gold-coated nanopore through the electrochemical polymerization of aniline on the pore surface [35]. Moreover, we have also demonstrated the occurrence of redox

reaction in the confined environment upon the addition of hydrogen peroxide in the electrolyte solution in contact with horseradish peroxidase enzyme-modified nanopores [37]. To broaden the scope and application spectrum of these nanoporous systems, the synthesis and anchoring of more complex functional molecules, e.g., oxidation-reduction (redox) sensitive moieties, on the pore surface constitutes a challenge for current techniques.

In living organisms, the majority of biological processes involves reversible oxidation and reduction (redox) reactions to store and release biological energy. The biologically relevant redox couples nicotinamide adenine dinucleotide (NAD^+/NADH) and nicotinamide adenine dinucleotide phosphate ($NADP^+$/NADPH), play a key role in cellular functions [38, 39]. Both contain the nicotinamide ring as a redox center on which oxidation and reduction processes occur. Oxidation of the substrate takes place by the removal of two hydrogen atoms (dehydrogenation) from the nicotinamide moiety. The oxidized nicotinamide (NAD^+ or $NADP^+$) accepts a hydride ion and subsequently transforms into the reduced nicotinamide (NADH or NADPH). The electrical charge on nicotinamide ring is dependent on the redox reaction, i.e., it is positively charged in oxidized and uncharged (neutral) in reduced form.

Previously, Imanishi and his co-workers have demonstrated the water permeation through porous membranes grafted with redox-responsive polymer brushes containing nicotinamide moieties [40]. Furthermore, Ishihara *et al*. investigated the insulin permeation rate via oxidation of nicotinamide moiety in a redox polymer grafted on a porous membrane [41]. Taking into account the redox-mediated switching of surface charge, we are interested in the possible modulation of

the transmembrane rectified ion flux by decorating nicotinamide units onto the inner surface and walls of the asymmetric nanopores.

We demonstrate the construction of a redox-sensitive nanofluidic diode based on single asymmetric nanopores. To achieve this goal, the chemical compounds 1-(4-aminobutyl)-3-carbamoylpyridinium (Nic-BuNH_2) and 3-carbamoyl-1-(2,4-dinitrophenyl)pyridiniumchloride (Nic-DNP) are synthesized and anchored onto the pore surface via carbodiimide coupling chemistry and Zincke reaction, respectively. The pore surface properties are tuned by exposing the modified pore to solutions of hydrogen peroxide (oxidant) and sodium dithionite (reductant), which leads to measurable changes in the electronic readout of the current–voltage (*I–V*) characteristics. The experimental results are also described theoretically by using a model based on the Poisson-Nernst-Planck equations.

2. Materials and methods

2.1 Materials

Polymer membranes of polyethylene terephthalate (PET) (Hostaphan RN 12, Hoechst) of thickness 12 μm were irradiated at the linear accelerator UNILAC (GSI, Darmstadt) with single swift heavy ions (Au) of kinetic energy 11.4 MeV/nucleon. Then, the ion tracked membranes were subjected to soft UV light irradiation on each side for 60 minutes. The UV irradiation process sensitized the latent tracks of heavy ions for the subsequent etching process.

All the chemicals and reagents were of analytical grade and used as received without further purification. *N*-(3-dimethylaminopropyl)-*N*-ethylcarbodiimide hydrochloride (EDC), pentafluorophenol (PFP), nicotinamide (Nic), 2,4-

dinitrochlorobenzene (DNCB), *tert*-butyl *N*-(4-aminobutyl)carbamate, hydrogen peroxide (H_2O_2), sodium dithionite, sodium bicarbonate, sodium hydroxide, potassium chloride and trifluoroacetic acid were purchased from Sigma-Aldrich, Schnelldorf, Germany.

2.2 Fabrication of single asymmetric nanopores

The latent ion damage tracks in polymer membranes were converted into conical nanopores through the asymmetric track-etching technique reported by Apel and co-workers [42]. A custom-made conductivity cell with three chambers was employed for the simultaneous fabrication of single-pore and multipore membranes. A single-shot membrane and a membrane irradiated with a flux of 10^7 ions/cm^2 were placed on both sides of the middle chamber of the conductivity cell and clamped tightly. The middle compartment contained apertures on both sides and was filled with an etching solution (9 M NaOH). The other two compartments were filled with an acidic etch stop solution (1 M KCl + 1 M HCOOH). Gold electrodes were inserted on both sides of the single-ion irradiated membrane and a potential of –1 V was applied across the membrane to monitor the etching process at room temperature. During this process, the current remained zero until the etchant permeated through the whole length of the membrane. After the breakthrough point, an increase in ionic current flowing through the nascent pore was observed. The etching process was stopped as the current reached to 0.5 ± 0.1 nA. Subsequently, the membranes were thoroughly washed with stopping solution in order to neutralize the etchant, followed by deionized water. The etched membranes were then dipped in deionized water overnight in order to remove the residual salts.

2.3 Synthesis of 1-(4-aminobutyl)-3-carbamoylpyridin-1-ium (Nic-BuNH$_2$) (6)

The chemical compounds 3-carbamoyl-1-(2,4-dinitrophenyl)pyridiniumchloride (Nic-DNP) referred as Zincke reagent (**3**) and 1-(4-aminobutyl)-3-carbamoylpyridin-1-ium (Nic-BuNH$_2$) (**6**) were synthesized according to the reported method with slight modifications (see supporting information for detail) [43, 44].

2.4 Functionalization of nanopore surface

2.4.1 Carbodiimide coupling chemistry

The carboxylic groups on the pore surface were first activated by exposing the single pore membrane to an ethanolic solution of *N*-(3-dimethyl-aminopropyl)-*N*-ethylcarbodiimide (EDC; 100 mM)/pentafluorophenol (PFP; 200 mM) for 1 h at room temperature. After activation, the samples were exposed to a solution of Nic-BuNH$_2$ (50 mM) prepared in ethanol and the reaction was allowed to occur overnight. Finally, the functionalized membrane was washed several times with ethanol followed by deionized water.

2.4.2 Zincke reaction

In this case, the carboxylic acid groups were first derivatized with ethylenediamine via EDP/PFP coupling chemistry. Subsequently, the aminated single pore membrane was exposed to a Nic-DNP (Zincke reagent; 40 mM) solution prepared in methanol for 24 h. Then, the membrane was washed carefully with methanol followed by deionized water to remove the physically adsorbed Nic-DNP molecules from the pore surface.

2.5 Current-voltage measurements

The carboxylated and Nic-modified single-pore membrane was fixed between the two halves of the conductivity cell. Both halves of the cell were filled with a 0.1

M KCl solution at pH 6. An Ag/AgCl electrode was inserted into each half-cell solution and a picoammeter/voltage source (Keithley 6487, Keithley Instruments, Cleveland, Ohio, USA) was used to apply the desired transmembrane potential and measure the ionic current across the membrane. In the case of the asymmetric nanopore, the ground electrode was placed on the base side of the pore. In order to record the *I–V* curves, a scanning triangle voltage signal from –2 to +2 V was used.

2.6 Reduction of nicotinamide

A solution of reductant $Na_2S_2O_4$ (20 mM) was prepared in an aqueous $NaHCO_3$ (50 mM). For the reduction of nicotinamide into dihydronicotinamide groups on the pore surface, the modified pore was exposed to $Na_2S_2O_4$ solution for 2 h. Then the pore was washed several times with water.

2.7 Oxidation of dihydronicotinamide

A 20 mM solution of oxidizing agent (H_2O_2) was prepared in water. Then, the pore was exposed to H_2O_2 solution for 2 h. During this time, the reduced dihydronicotinamide was oxidized back to nicotinamide moieties on the pore surface. The pore was washed with deionized water before *I–V* measurement.

2.8 Theoretical modeling

The experimental *I–V* curves can be described in terms of a theoretical model previously developed based on the Poisson and Nernst-Planck (PNP) equations

$$\nabla^2\phi = \frac{F}{\varepsilon}\left(c_{\mathrm{Cl}^-} - c_{\mathrm{K}^+}\right) \tag{1}$$

$$\nabla \cdot \vec{J}_\mathrm{i} = -\nabla \cdot \left[D_\mathrm{i}\left(\nabla c_\mathrm{i} + z_\mathrm{i} c_\mathrm{i} \nabla\phi\right)\right] = 0\,,\ \mathrm{i} = \mathrm{K}^+, \mathrm{Cl}^- \tag{2}$$

where D_i, c_i, $\vec{J}_\mathrm{i}$, and z_i are, respectively, the diffusion coefficient, the local concentration, the flux and the charge number of ion *i* ($i = K^+$ and Cl^-), and ε and ϕ are the electrical permittivity and the local electric potential of the solution. Integration of

Equations (1)-(2) permits the calculation of the ionic fluxes at a given voltage. Once the ionic fluxes have been calculated, the electric current passing through any arbitrary section of radius a in the pore

$$I = \sum_i z_i F \pi a^2 J_i \,. \tag{3}$$

can be obtained. Additional details can be found in Reference [45].

Assuming a conical geometry for the pore and infinite dilution values for the diffusion coefficients, the unknown model parameters are the diameters of the pore base and tip, D and d, respectively, and the concentration of fixed charges on the pore surface, σ (in elementary charges per square nanometer). In our experiments, the model parameters are assessed according to the following scheme. First, the pore base diameter is determined using SEM techniques with a membrane sample containing a large number of pores (ca. 10^7 pores cm^{-2}) which was etched at the same time as the single pore sample. The tip diameter is calculated from the *I–V* curve of the as-prepared pore sample separating two 1 M KCl solutions. Under these conditions, the electrolyte ions screen the surface charges ($\sigma = 0$) leading to a quasi-linear I–V curve. Parameters D and d are assumed to remain constant for a given sample after successive modifications of the pore surface charges. With this assumption, the only unknown parameter (σ) is calculated by fitting the theoretical results to the experiments.

It must be mentioned that the 1-dimensional PNP model used here contains a number of approximations: the electrolyte is treated as an ideal solution, ignoring the finite size of ions, diffusion boundary layers at the membrane-solution interfaces that might lead to additional potential drops are not included in the model, and the ionic diffusion coefficients within the nanopore are similar to those in the bathing solutions. In addition, the shape of the nanopore might not be exactly conical and the surface

charge density could not be homogeneously distributed along the pore, as assumed in the model. Therefore, the conclusions concerning the nanopore structure obtained from the fitting procedure should be valid only qualitatively. While more realistic 2-D models and simulations handling the electrostatic correlations beyond the mean field approximation have been reported [46, 47], the pore geometry and the distribution of fixed charges along the pore cannot be unambiguously determined and these models include more unknown parameters than the simple 1-D approach used here.

3. Results and discussion

In PET membranes, the fabrication of asymmetric nanopores was realized via the track-etching method. Swift heavy ion irradiation and chemical etching of ion tracks leads to the generation of carboxylic acid (–COOH) groups on the pore surface. These groups served as starting units to further tune the chemical characteristics of the surface. The chemical compounds, 1-(4-aminobutyl)-3-carbamoylpyridin-1-ium (Nic–$BuNH_2$) and 3-carbamoyl-1-(2,4-dinitrophenyl)pyridinium (Nic–DNP) having nicotinamide moiety were synthesized (Scheme 1A). The Zincke reagent (**3**) was synthesized by reacting nicotinamide (**1)** and 2,4-dinitrochlorobenzene (**2)**. The Zincke reagent **3** was then coupled with tert-butyl-4-aminobutylcarbamate (**4)** to prepare the Nic-BuNHBoc (**5**). The boc group was removed by treating compound **5** with trifluoroacetic acid to obtain Nic-$BuNH_2$ (**6**).

The as-prepared pores are used to covalently couple the carboxyl groups and amino groups of Nic–$BuNH_2$ on the channel surface through EDC/PFP coupling chemistry (Scheme 1B(a)). The Nic–DNP molecules were decorated on the EDA-modified pore surface using Zincke reaction (Scheme 1B(b)). The presence of

nicotinamide moiety onto the pore surface was confirmed by measuring the *I–V* curves before and after chemical modification. For recording the *I–V* curves, the single-pore membrane (as-prepared/modified) was assembled between the two compartments of a conductivity cell. The electrolyte solution (0.1 M KCl) prepared in tris buffer (10 mM, pH 6.0) was filled in both compartments of the conductivity cell on either side of the membrane. The electrodes are arranged in such a way that high and low ionic currents were recorded for the positive and negative voltages, respectively.

It is well-known that conical nanopores exhibit cation selectivity and current rectification phenomena. This means that under an applied potential cations preferentially flow from the tip opening towards the base opening of the pore due to the presence of negatively charged carboxylate ($–COO^-$) groups on the nanopore surface [9-11].

Figure 1A shows the *I–V* curves of a single asymmetric nanopore pore before and after the immobilization of nicotinamide moieties using EDP/PFP coupling chemistry. The modification process resulted in the switching of pore surface charge from negative to positive due to the presence of positively charged quaternary pyridinium units. This fact caused a reverse in the current rectification, i.e., the NicBu-modified pore preferentially transported anions from the tip to the base, as shown by the reverse *I–V* curve obtained compared with the case of the as-prepared pore of Figure 1A. This confirmed the successful attachment of nicotinamide moieties on the pore surface and walls. The theoretical results of Figure 1B were calculated following the procedure depicted in section 2.8 to determine the pore base (D = 400 nm) and tip (d = 24 nm) diameters. The concentrations of surface charge where σ = –0.2 e/nm^2 for the as-prepared pore and σ = 0.12 e/nm^2 for the NicBu-modified pore,

where *e* is the elementary charge. These results indicate a partial substitution (~60%) of the original carboxylate groups of the as-prepared pore by the nicotinamide moieties of the NicBu-modified pore.

Once the nanopore surface was successfully functionalized with nicotinamide moieties, we proceeded to study the redox reactions inside the confined environment. The immobilized nicotinamide moieties were in oxidized state (quaternary pyridinium form) and the net charge on pore surface was positive, as evidenced from the current rectification reversal. The reduction of nicotinamide moieties was performed by replacing the electrolyte solution (100 mM KCl) used in the *I*−*V* measurements with sodium dithionite ($Na_2S_2O_4$) prepared in sodium bicarbonate solution. The pore remained in contact with the reductant solution in dark for a time period. During the course of the reduction process, the oxidized (positively charged) pyridinium ring of nicotinamide was converted to 1,4-dihydropyridine (uncharged/ neutral) form, resulting in the loss of pore surface charges, as shown in Figure 2A. To avoid any interference from the reducing agent, the reductant solution was replaced by pure 0.1 KCl in both half cells for each *I*−*V* measurement. Moreover, the reproducibility of the redox system was validated by performing the same experiment on two single pore membrane samples (data not shown here).

Figure 2B depicts the *I*−*V* curves of the nanopore with nicotinamide moiety in the oxidized and reduced states. Upon reduction, the pore becomes nonselective due to the existence of uncharged dihydronicotinamide groups on the surface, as evidenced from the linear *I*−*V* characteristics (the net surface charge on the pore walls was then zero. From the *I*−*V* curves (1^{st} cycle), the reduction process switched the nanopore from an "*ON*" state characterized by a high rectified ion flux to an "*OFF*" state with a low non-rectified current.

The dihydronicotinamide can be reoxidized back to nicotinamide in successive cycles by exposing the modified pore to a solution of an oxidizing agent. We employed hydrogen peroxide (H_2O_2) for the oxidation of dihydronicotinamide. The oxidation process resulted in the generation of positive charges on the pore walls. Eventually, the pore became anion-selective and rectified the ion current as evidenced in the $I-V$ curves (2^{nd} cycle). This procedure was repeated again, giving the results of the $I-V$ curves (3^{rd} cycle). The redox-sensitive interconversion of nicotinamide ↔ dihydronicotinamide is responsible for the polarity of the pore surface, which in turn affects the membrane permselectivity. This fact suggested that the redox controlled reversible nicotinamide/dihydronicotinamide interconversion provided a chemical tool to modulate the electronic readout of ionic current flowing through the nanopore, as shown in the experiments of Figure 2B.

Figure 2C shows the results obtained with the theoretical model in the successive reversible nicotinamide/dihydronicotinamide interconversion cycles. The pore diameters used in the calculations (D = 400 nm and d = 24 nm) were the same as in Figure 1B. The calculated surface charge densities (see the insets in the curves) reveal a partial recovery of the positive charges after the successive redox cycles. Progressive pore reutilization along several cycles decreases the effective number of charged groups leading to decreasing values of sigma, probably because of partial regeneration.

The second approach employed to immobilize nicotinamide moieties on the pore surface was based on Zincke reaction (Scheme 1B(b)) [48, 49]. To this end, the carboxylic acid groups on the as-prepared pore surface of a new sample were first derivatized with ethylediamine (EDA) using carbodiimide coupling chemistry. The presence of amine groups on the pore surface was confirmed by recording the $I-V$

curve. The EDA-modified pore exhibited anion-selectivity, as reflected from its reversed $I-V$ curve (Figure 3A). Subsequently, the EDA-modified pore was exposed to a methanolic solution of Nic–DNP compound (Zincke reagent) [49]. During the course of reaction, the amine groups on the pore surface acted as nucleophile and incorporated at the 6-position of nicotinamide group of Nic-DNP compound, resulting in the generation of 2,4-dinitroaniline. The pore functionalized through Zincke reaction, in the following denoted as "Nic-modified pore", still exhibited reversed current rectification due to the existence of the positively charged nicotinamide moiety. When Nic-modified pore was exposed to reductant solution, the nicotinamide moiety transformed into its complementary reduced neutral dihydronicotinamide, as suggested by the linear $I-V$ characteristic of the pore (Figure 3A). The theoretical results of Figure 3B were calculated again following the procedure described in section 2.8 and resulted in the pore diameters D = 240 nm and d = 24 nm and the surface charge densities indicated in the figure inset. In this case, the model results suggest the substitution of the amine groups by the nicotinamide groups of the pore surface.

We also performed a control experiment to demonstrate the success of Zincke reaction, the switching of pore surface polarity, and the concomitant changes in the current rectification observed in Figure 3 due to the reduction of nicotinamide. For this purpose, another pore modified with EDA was exposed to a solution of reducing agent under the same experimental conditions of Figure 3. $I–V$ curves in Figure 4 did not show any significant change in the current rectification on exposure to reductant solution. These experimental results further confirmed the nicotinamide immobilization on the pore surface via Zincke reaction and the subsequent reduction inside the confined geometry.

4. Conclusions

In summary, we have demonstrated the fabrication of a redox-sensitive nanofluidic diode whose transport properties can be reversibly tuned via oxidation and reduction processes occurring inside the pore. The chemical compounds Nic–$BuNH_2$ and Nic–DNP were synthesized and functionalized on the pore surface via carbodiimide coupling chemistry and Zincke reaction, respectively. After the nicotinamide functionalization, the surface polarity was switched from negative to positive, resulting in the reverse of the current rectification characteristic of the nanopore. The reduction of nicotinamide into dihydronicotinamide (neutral) moieties led to the loss of current rectification and the pore behaved like an ohmic resistor. The rectification behaviour was subsequently recovered by re-oxidation of dihydronicotinamide into nicotinamide moieties. In summary, the redox reactions allowed us to reversibly switch the nanopore inner environment from hydrophilic and conducting ("*ON*" state) to a hydrophobic and nonconducting ("*OFF*" state). Model calculations allow for the determination of the key transport parameters of the functionalized pores.

Acknowledgements

M.A., S.N. and W.E. acknowledge the funding from the Hessen State Ministry of Higher Education, Research and the Arts, Germany, under the LOEWE project iNAPO. P. R. and S. M. acknowledge financial support by the Generalitat Valenciana (Program of Excellence Prometeo/GV/0069), the Spanish Ministry of Economic Affairs and Competitiveness (MAT2015-65011-P), and FEDER. I.A. and C.M.N.

1 acknowledge financial support through the Helmholtz programme BioInterfaces in
2 Technology and Medicine. The authors are also thankful to Prof. C. Trautmann,
3 Department of Materials Research from GSI, for support with irradiation experiments.
4

References

[1] B. Hille, Ionic channels of excitable membranes, 3rd ed., Sunderland, MA: Sinauer Associates Inc.; 2001.

[2] A. Alcaraz, E.M. Nestorovich, M. Aguilella-Arzo, V.M. Aguilella, S.M. Bezrukov, Salting out the ionic selectivity of a wide channel: The asymmetry of OmpF, Biophys J, 87(2004) 943-57.

[3] A. Alcaraz, P. Ramirez, E. Garcia-Gimenez, M.L. Lopez, A. Andrio, V.M. Aguilella, A pH-tunable nanofluidic diode: Electrochemical rectification in a reconstituted single ion channel, J Phys Chem B, 110(2006) 21205-9.

[4] H. Bayley, O. Braha, L.Q. Gu, Stochastic Sensing with Protein Pores, Adv Mater, 12(2000) 139-42.

[5] H. Bayley, P.S. Cremer, Stochastic sensors inspired by biology, Nature, 413(2001) 226-30.

[6] C. Dekker, Solid-state nanopores, Nat Nanotechnol, 2(2007) 209-15.

[7] X. Hou, W. Guo, L. Jiang, Biomimetic smart nanopores and nanochannels, Chem Soc Rev, 40(2011) 2385-401.

[8] Z.S. Siwy, S. Howorka, Engineered voltage-responsive nanopores, Chem Soc Rev, 39(2010) 1115-32.

[9] Z.S. Siwy, Ion-Current Rectification in Nanopores and Nanotubes with Broken Symmetry, Adv Funct Mater, 16(2006) 735-46.

[10] P. Ramirez, V. Gomez, J. Cervera, B. Schiedt, S. Mafe, Ion transport and selectivity in nanopores with spatially inhomogeneous fixed charge distributions, J Chem Phys, 126(2007) 194703.

[11] P. Ramirez, S. Mafe, A. Alcaraz, J. Cervera, Modeling of pH-switchable ion transport and selectivity in nanopore membranes with fixed charges, J Phys Chem B, 107(2003) 13178-87.

[12] A. Wolf, Z. Siwy, Y.E. Korchev, N. Reber, R. Spohr, Ion current fluctuations in artificial ion-track pores - Power spectrum and generalized entropy, Cell Mol Biol Lett, 4(1999) 553-65.

[13] Q. Liu, K. Xiao, L. Wen, H. Lu, Y. Liu, X.-Y. Kong, et al., Engineered Ionic Gates for Ion Conduction Based on Sodium and Potassium Activated Nanochannels, J Am Chem Soc, 137(2015) 11976-83.

[14] M. Ali, S. Nasir, P. Ramirez, J. Cervera, S. Mafe, W. Ensinger, Calcium Binding and Ionic Conduction in Single Conical Nanopores with Polyacid Chains: Model and Experiments, ACS Nano, 6(2012) 9247-57.

[15] M. Ali, I. Ahmed, P. Ramirez, S. Nasir, C.M. Niemeyer, S. Mafe, et al., Label-Free Pyrophosphate Recognition with Functionalized Asymmetric Nanopores, Small, 12(2016) 2014-21.

[16] M. Ali, S. Nasir, W. Ensinger, Bioconjugation-induced ionic current rectification in aptamer-modified single cylindrical nanopores, Chem Commun, 51(2015) 3454-7.

[17] M. Ali, B. Schiedt, R. Neumann, W. Ensinger, Biosensing with Functionalized Single Asymmetric Polymer Nanochannels, Macromol Biosci, 10(2010) 28-32.

[18] I. Vlassiouk, T.R. Kozel, Z.S. Siwy, Biosensing with Nanofluidic Diodes, J Am Chem Soc, 131(2009) 8211-20.

[19] I. Vlassiouk, C.D. Park, S.A. Vail, D. Gust, S. Smirnov, Control of nanopore wetting by a photochromic spiropyran: A light-controlled valve and electrical switch, Nano Lett, 6(2006) 1013-7.

[20] G.L. Wang, A.K. Bohaty, I. Zharov, H.S. White, Photon gated transport at the glass nanopore electrode, J Am Chem Soc, 128(2006) 13553-8.

[21] M. Ali, S. Nasir, P. Ramirez, I. Ahmed, Q.H. Nguyen, L. Fruk, et al., Optical Gating of Photosensitive Synthetic Ion Channels, Adv Funct Mater, 22(2012) 390-6.
[22] S. Nasir, P. Ramirez, M. Ali, I. Ahmed, L. Fruk, S. Mafe, et al., Nernst-Planck Model of Photo-Triggered, pH-Tunable Ionic Transport through Nanopores Functionalized with ``Caged'' Lysine Chains, J Chem Phys, 138(2013) 034709.
[23] M. Ali, S. Mafe, P. Ramirez, R. Neumann, W. Ensinger, Logic Gates Using Nanofluidic Diodes Based on Conical Nanopores Functionalized with Polyprotic Acid Chains, Langmuir, 25(2009) 11993-7.
[24] M. Ali, P. Ramirez, S. Mafe, R. Neumann, W. Ensinger, A pH-Tunable Nanofluidic Diode with a Broad Range of Rectifying Properties, ACS Nano, 3(2009) 603-8.
[25] B. Yameen, M. Ali, R. Neumann, W. Ensinger, W. Knoll, O. Azzaroni, Synthetic Proton-Gated Ion Channels via Single Solid-State Nanochannels Modified with Responsive Polymer Brushes, Nano Lett, 9(2009) 2788-93.
[26] B. Yameen, M. Ali, R. Neumann, W. Ensinger, W. Knoll, O. Azzaroni, Ionic Transport Through Single Solid-State Nanopores Controlled with Thermally Nanoactuated Macromolecular Gates, Small, 5(2009) 1287-91.
[27] S. Nasir, M. Ali, W. Ensinger, Thermally controlled permeation of ionic molecules through synthetic nanopores functionalized with amine-terminated polymer brushes, Nanotechnology, 23(2012) 225502.
[28] X. Hou, F. Yang, L. Li, Y.L. Song, L. Jiang, D.B. Zhu, A Biomimetic Asymmetric Responsive Single Nanochannel, J Am Chem Soc, 132(2010) 11736-42.
[29] W. Guo, H.W. Xia, L.X. Cao, F. Xia, S.T. Wang, G.Z. Zhang, et al., Integrating Ionic Gate and Rectifier Within One Solid-State Nanopore via Modification with Dual-Responsive Copolymer Brushes, Adv Funct Mater, 20(2010) 3561-7.
[30] E. Aznar, M. Oroval, L. Pascual, J.R. Murguía, R. Martínez-Máñez, F. Sancenón, Gated Materials for On-Command Release of Guest Molecules, Chem Rev, 116(2016) 561-718.
[31] Q. Chen, K. McKelvey, M.A. Edwards, H.S. White, Redox Cycling in Nanogap Electrochemical Cells. The Role of Electrostatics in Determining the Cell Response, J Phys Chem C, 120(2016) 17251-60.
[32] J. Elbert, F. Krohm, C. Rüttiger, S. Kienle, H. Didzoleit, B.N. Balzer, et al., Polymer-Modified Mesoporous Silica Thin Films for Redox-Mediated Selective Membrane Gating, Adv Funct Mater, 24(2014) 1591-601.
[33] C. Ma, W. Xu, W.R.A. Wichert, P.W. Bohn, Ion Accumulation and Migration Effects on Redox Cycling in Nanopore Electrode Arrays at Low Ionic Strength, ACS Nano, 10(2016) 3658-64.
[34] S.A. Miller, C.R. Martin, Redox Modulation of Electroosmotic Flow in a Carbon Nanotube Membrane, J Am Chem Soc, 126(2004) 6226-7.
[35] G. Pérez-Mitta, W.A. Marmisollé, C. Trautmann, M.E. Toimil-Molares, O. Azzaroni, Nanofluidic Diodes with Dynamic Rectification Properties Stemming from Reversible Electrochemical Conversions in Conducting Polymers, J Am Chem Soc, 137(2015) 15382-5.
[36] K. Zhang, X. Feng, X. Sui, M.A. Hempenius, G.J. Vancso, Breathing Pores on Command: Redox-Responsive Spongy Membranes from Poly(ferrocenylsilane)s, Angew Chem Int Ed, 53(2014) 13789-93.
[37] M. Ali, M.N. Tahir, Z. Siwy, R. Neumann, W. Tremel, W. Ensinger, Hydrogen Peroxide Sensing with Horseradish Peroxidase-Modified Polymer Single Conical Nanochannels, Anal Chem, 83(2011) 1673-80.

[38] W. Xia, Z. Wang, Q. Wang, J. Han, C. Zhao, Y. Hong, et al., Roles of NAD(+) / NADH and NADP(+) / NADPH in cell death, Curr Pharm Des, 15(2009) 12-9.
[39] W. Ying, NAD+/NADH and NADP+/NADPH in cellular functions and cell death: regulation and biological consequences, Antioxid Redox Signal, 10(2008) 179-206.
[40] Y. Ito, S. Nishi, Y.S. Park, Y. Imanishi, Oxidoreduction-Sensitive Control of Water Permeation through a Polymer Brushes-Grafted Porous Membrane, Macromolecules, 30(1997) 5856-9.
[41] K. Ishihara, M. Kobayashi, I. Shionohara, Control of insulin permeation through a polymer membrane with responsive function for glucose, Makromol Chem Rapid Commun, 4(1983) 327-31.
[42] P.Y. Apel, Y.E. Korchev, Z. Siwy, R. Spohr, M. Yoshida, Diode-Like Single-Ion Track Membrane Prepared by Electro-Stopping, Nucl Instrum Methods Phys Res, Sect B, 184(2001) 337-46.
[43] S.A. Löw, I.M. Löw, M.J. Weissenborn, B. Hauer, Enhanced Ene-Reductase Activity through Alteration of Artificial Nicotinamide Cofactor Substituents, ChemCatChem, 8(2016) 911-5.
[44] M.A. Mateos-Timoneda, M.C. Lok, W.E. Hennink, J. Feijen, J.F.J. Engbersen, Poly(amido amine)s as Gene Delivery Vectors: Effects of Quaternary Nicotinamide Moieties in the Side Chains, ChemMedChem, 3(2008) 478-86.
[45] J. Cervera, B. Schiedt, R. Neumann, S. Mafe, P. Ramirez, Ionic Conduction, Rectification, and Selectivity in Single Conical Nanopores, J Chem Phys, 124(2006) 104706.
[46] D. Constantin, Z. Siwy, Poisson-Nernst-Planck Model of Ion Current Rectification through a Nanofluidic Diode, Phys Rev E 76(2007), 041202.
[47] D. Boda, D. Gillespie, Steady-State Electrodiffusion from the Nernst-Planck Equation Coupled to Local Equilibrium Monte Carlo Simulations, J Chem Theor Comput 8(2012), 824.
[48] J.F.J. Engbersen, A. Koudijs, H.C. Van der Plas, Metal-1,10-phenanthroline-linked dihydronicotinamides as models for the NADH-alcohol dehydrogenase coenzyme-enzyme couple, J Org Chem, 55(1990) 3647-54.
[49] B.V. Plapp, C. Woenckhaus, G. Pfleiderer, Evaluation of N1-(ω-bromoacetamidoalkyl)nicotinamides as inhibitors of dehydrogenases, Arch Biochem Biophys, 128(1968) 360-8.

Figures and Legends

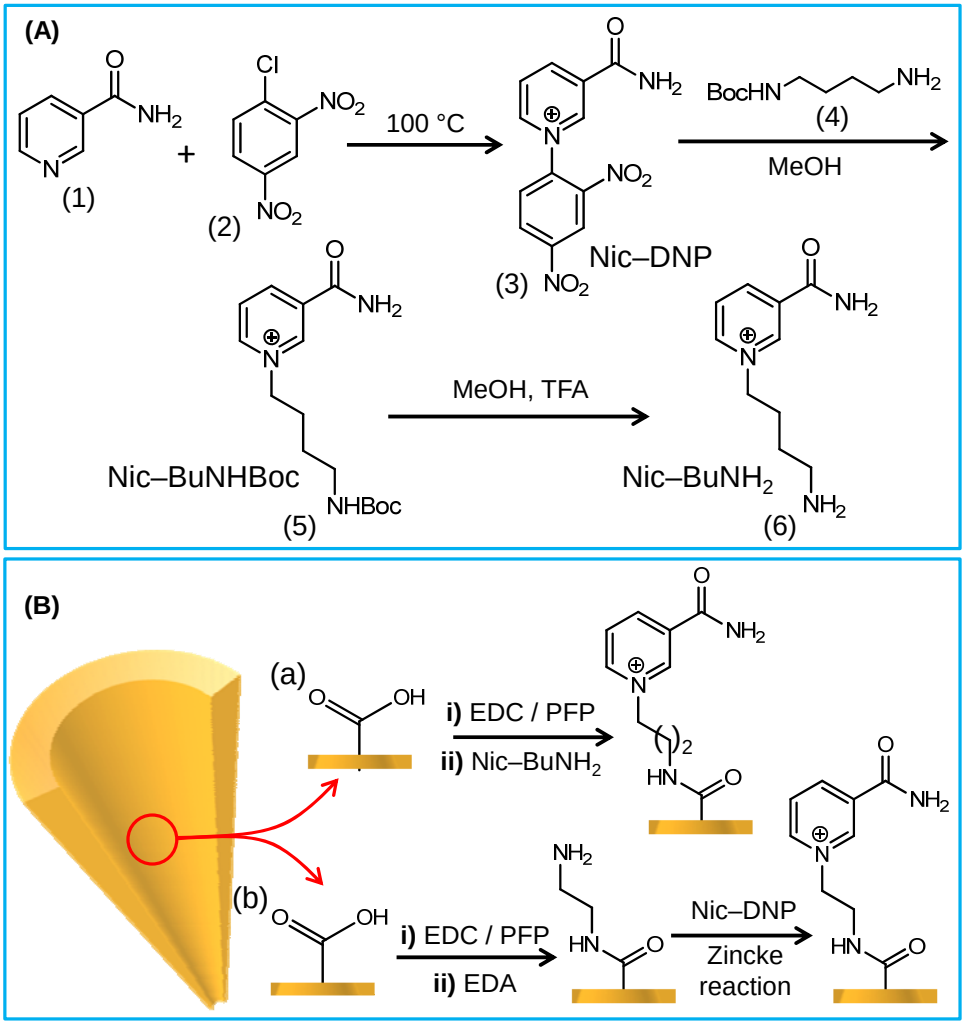

Scheme 1. (A) Reaction scheme for the synthesis of Nic–DNP (3) and Nic–$BuNH_2$ (6) compounds. (B) The functionalization of the pore surface carboxylic acid groups with Nic–$BuNH_2$ molecules via carbodiimide coupling chemistry (a) and immobilization of Nic–DNP moieties through Zincke reaction (b).

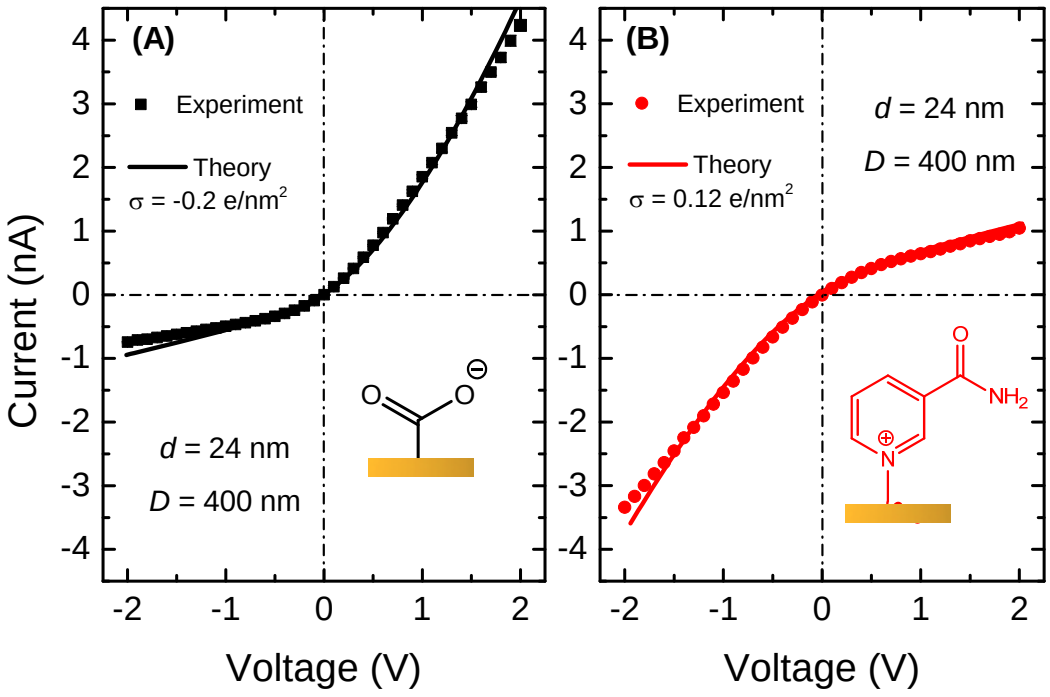

Figure 1. Experimental and theoretical *I–V* curves of single conical nanopore measured in aqueous 0.1M KCl (pH 6.0) with carboxylate groups (A) and nicotinamide moieties (B) on the pore surface.

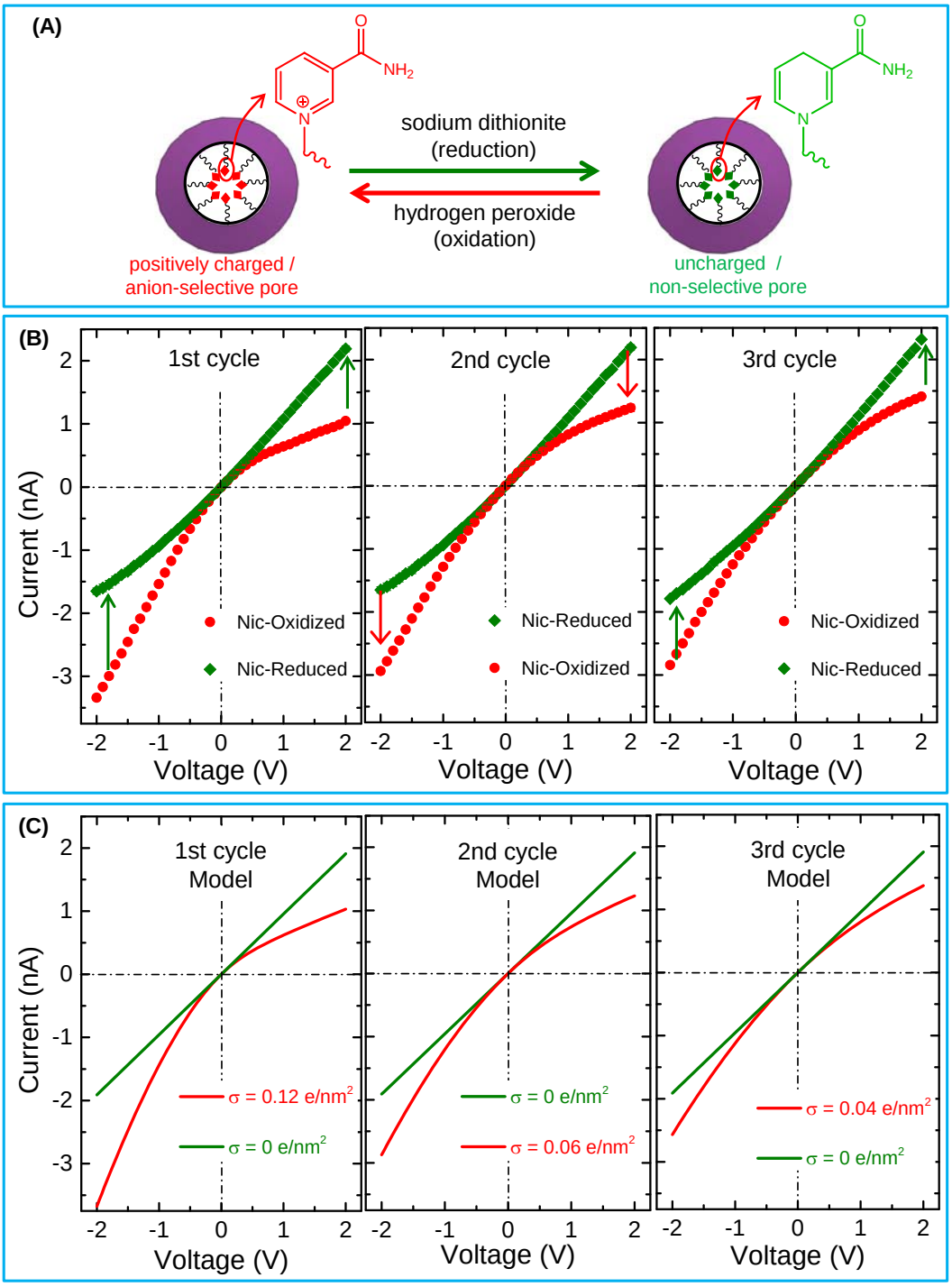

Figure 2. (A) Scheme for the oxidation and reduction of nicotinamide moieties on the inner pore walls. (B) Experimental *I–V* curves of the NicBu-modified pore exhibiting the reversible switching between the oxidized (positively charged) and reduced (uncharged) states of nicotinamide moieties measured in aqueous 0.1M KCl (pH 6.0), separately. (C) Theoretical *I–V* curves corresponding to the experimental data. Pore diameters *D* and *d* were the same as those in Figure 1B.

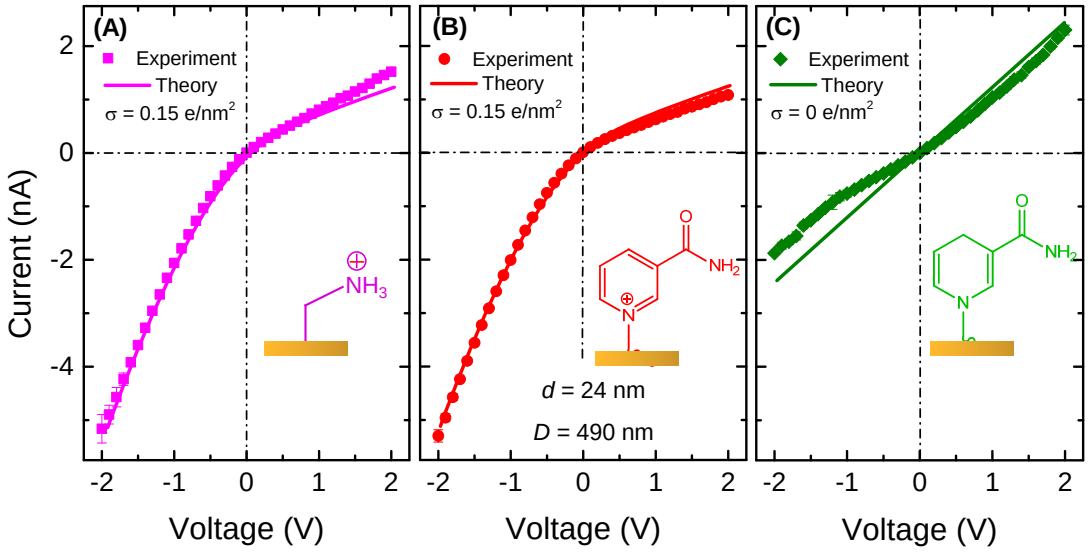

Figure 3. Experimental and theoretical *I–V* curves of single conical nanopore containing the amine groups (A) and the nicotinamide moieties in the oxidized (B) and reduced (C) states measured in an aqueous 0.1M KCl (pH 6.0) solution, separately.

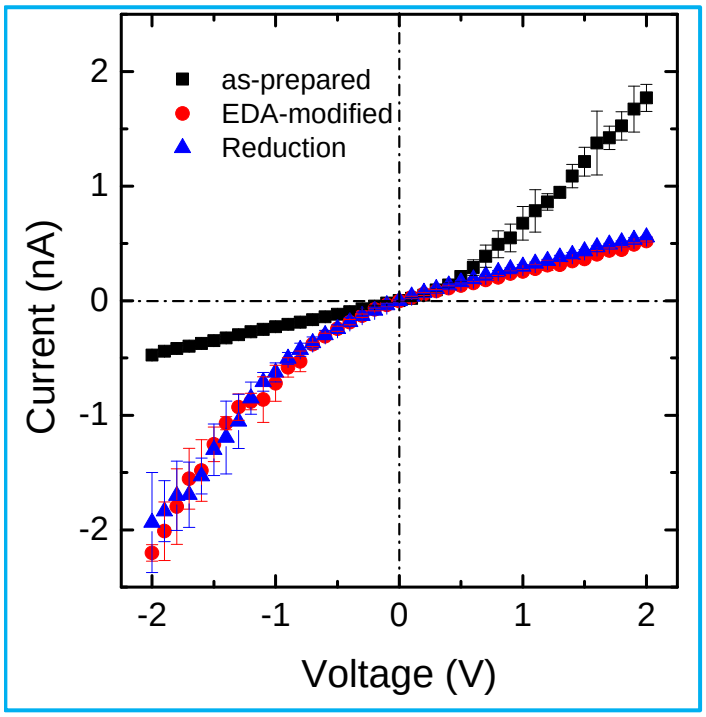

Figure 4. *I–V* curves of as-prepared pore and EDA-modified conical nanopore after exposure to dithionite solution measured in aqueous 0.1 M KCl (pH 6.0) solution.